

Effect of ultrasonic processing on a direct chill cast AA6082 aluminium alloy

G. Salloum-Abou-Jaoude¹, D. G. Eskin¹, C. Barbatti², P. Jarry², M. Jarrett², Z. Fan¹

¹BCAST, Brunel University, Uxbridge, Middlesex UB8 3PH, UK

²Constellium, Parc Economique Centr'alp, CS10027, Voreppe, 38341 cedex, France

Keywords: DC casting, ultrasonic processing, AA6082, grain refiner, CET, grain size, microstructure, nuclei

Abstract

For many years now, ultrasonic melt treatment (UST) has proven itself to promote grain refinement in aluminium alloys. The current work presents cavitation-aided grain refinement obtained on commercial AA6082 DC-cast billets. Grain refinement was achieved while applying UST in the crucible away from the sump, prior to casting. Since in high strength alloys, Zr and Ti are commonly present as alloying elements for anti-recrystallization and corrosion resistance properties, their as well as UST parameters influence on the microstructure are studied and presented. Primary $\text{Al}_3(\text{Zr}_{1-x-y}, \text{Ti}_x, \text{Si}_y)$ intermetallics were found in the centre of the α -Al grains. This suggests that UST may have forced the nucleation and refinement of primary intermetallics influencing the subsequent solidification process when $\text{Al}_3(\text{Zr}_{1-x-y}, \text{Ti}_x, \text{Si}_y)$ act as nucleation sites.

Introduction

Direct chill casting of aluminium alloys, commonly known as DC casting, is a technology that provides sound cylindrical billets or flat ingots required for extrusion, forging, or rolling in the automotive and aerospace aluminium industry [1].

Control of grain size in DC-cast billets and ingots is essential to prevent hot tearing linked to the inadequate compensation of the solidification shrinkage and mechanical properties of the semi-solid material [2], shrinkage porosity resulting from insufficient feeding of the gaps between the solid dendrites [3], cold cracking is related to low ductility of the as-cast material [4], and macrosegregation in the billet [5], [6].

As a result, fine and uniform, equiaxed grain structure is highly beneficial for industrial casting processes. Other than giving better properties to the cast metal, it facilitates the subsequent mechanical working [7], [8]. A full columnar to equiaxed transition (CET) [9], [10] is required to achieve a uniform equiaxed structure. Many methods are available to trigger CET and reach a fully equiaxed microstructure. A common industrial practice is to add grain refiner rods containing potent nucleant particles like Al-Ti-B and Al-Ti-C to promote the formation of a fine, uniform and equiaxed grain structure [11]. Other methods to refine the microstructure involve using a pulse magnetic field (PMF) [12], pulse magneto-oscillation (PMO) [13], [14], electric current pulse (ECP) [15]–[17], high shearing [18], and ultrasonic melt treatment (UST) [19]–[22].

The challenge in applying an external field or mechanical shearing during solidification in DC casting is purely technical. Moving away from the solidification domain (sump) during DC casting is advantageous from an industrial point of view as it increases the productivity of treating larger volumes and reduces the risk of technical failures. It has been shown that high shearing can be applied before casting to refine Fe bearing intermetallics that can serve as nuclei for α -Al grains [23]. Similarly, UST has been also applied prior to casting in permanent moulds on Zr-containing aluminium alloys to force the nucleation of Al_3Zr intermetallics and promote CET of α -Al grains reaching a very fine grain structure [20]. In this work we present results obtained on the refinement of a commercial AA6082 alloy obtained by applying UST prior to casting in a DC-casting simulator.

Experimental Procedure

DC-casting simulator

In order to perform relatively easy and fast DC-casting experiments, a DC-casting simulator was used. The DC-simulator consists of a tapered steel sleeve (64 mm bottom diameter and 75 mm top diameter) resting on a steel base, surrounded by resistance heaters that will preheat it 20 °C above the pouring temperature (T_p) before each experiment (Figure 1-a). The sleeve is well isolated to ensure that at the moment of pouring the solidification will start at the steel base at the bottom of the sleeve. When the steel sleeve is full of liquid aluminium alloy, the water nozzles are switched on and a constant pulling rate of 150 mm/min is applied moving the sleeve downward through the quench zone where the water nozzles come in direct contact with the steel mould solidifying the aluminium indirectly from the sides simulating the solidification

during a standard DC casting (Figure 1-c). The final cylindrical shaped billet can be seen in Figure 1-c.

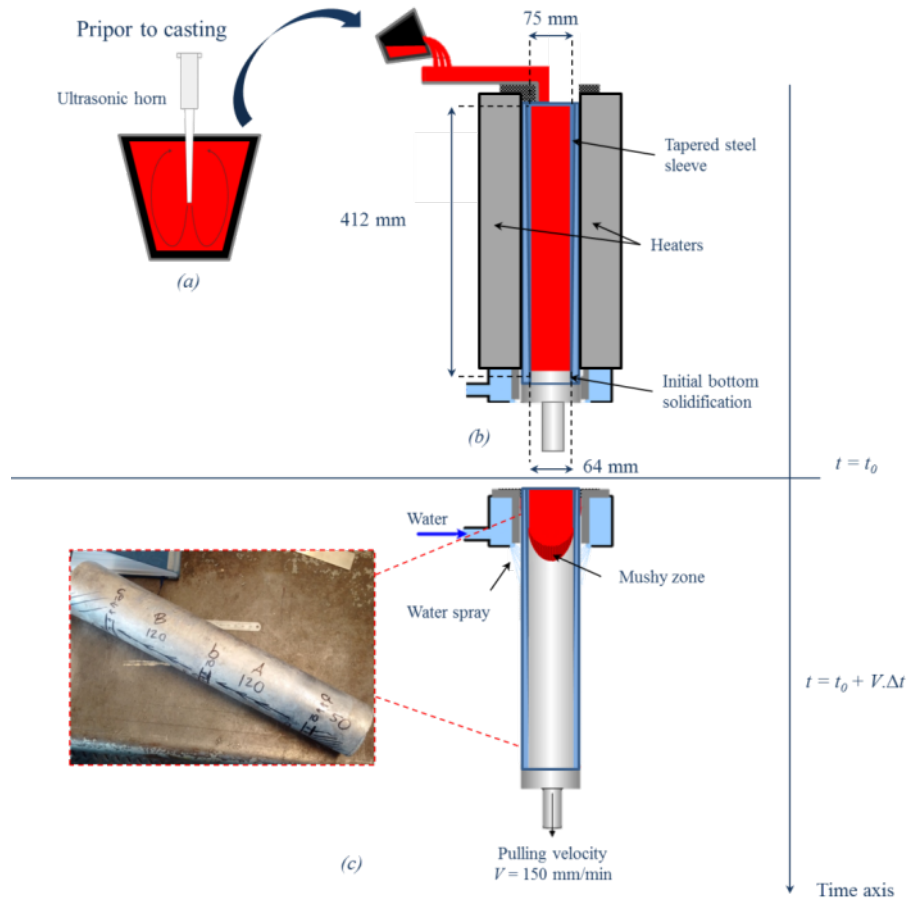


Figure 1: Sketch of the DC-casting simulator experimental setup as a function of the experimentation time t . (a) The UST processing is applied in the crucible prior to casting, (b) then poured entirely into the steel sleeve at $t = t_0$ before (c) starting the constant pulling of the sleeve down to the quench zone shaping the final billet (left photo in c)

Melt preparation and treatment

To study the effect of ultrasonic processing on the microstructural refinement of an AA6082 aluminium alloy, approximately 100 kg of AA6082 were prepared by melting commercial purity aluminium (99.98 wt.%) and adding to it precise amounts of Al – 20 wt% Si, Al– 10 wt% Fe, Al–20 wt% Mn, 100 wt% Mg, 100 wt% Zn, Al–50 wt% Cu, Al–10 wt% Ti and Al–10 wt% Zr master alloys.

The AA6082 alloy cast was analysed with a FOUNDRY-MASTER Pro optical emission spectrometer (OES) and the composition achieved was in the range of a commercial AA6082 as shown in Table I.

Table I: Aluminium Association 6082 composition range

Element	Si	Fe	Cu	Mn	Mg	Cr	Zr	Ti	Al
Composition range (wt %)	0.7-1.3	0.0-0.5	0.0-0.1	0.4-1.0	0.6-1.2	0.0-0.25	0.0-0.05	0.0-0.1	balance

From the 100 kg batch of AA6082, small 4 kg charges were put in graphite–clay crucibles and remolten in an electrical furnace. Variants were cast by adding small amounts of Al – 10 wt% Ti and Al – 10 wt% Zr master alloys to the re-molten AA6082 to increase the amount of Ti and/or Zr.

In some experiments, ultrasonic treatment (UST) was applied in the crucible prior to casting to study the effect of ultrasound cavitation on the solidified microstructure. UST was applied in a temperature range well above the α -Al nucleation temperature so that ultrasonic cavitation would not fragment the α -Al dendrites [19]. Experiments were performed with a magnetostrictive transducer at a resonance frequency of 17.5 kHz, amplitude 25 μ m and the input power at the generator 3.5–4.0 kW (ultrasonic equipment is made by Reltec, Yekaterinburg, Russia). A horn was made of niobium.

Moreover, Al-5Ti-1B commercial grain refiner was also added for some experiments. The melt was poured in the DC-casting simulator at a pouring temperature (T_p) of 700 °C. Table II shows the list of experiments performed in this study.

Table II: List of DC-casting simulator experiments

Exp. Name	Base alloy	Zr (wt.%)	Ti (wt.%)	Al-5Ti-1B (wt.%)	UST	UST ΔT (°C)	T_p (°C)
S1	6082	0.05	0.04	-	-	-	700
S2	6082	0.05	0.04	0.1	-	-	700
S3	6082	0.2	0.10	-	-	-	700
S4	6082	0.2	0.04	-	Yes	750-705	700
S5	6082	0.2	0.1	-	Yes	750-705	700

Sample preparation and grain size measurement

After casting, 2 cm thick disk slices were cut at mid-length of the billets for microstructure analysis (marked as “b” in the photo in Figure 1-c). Samples were cut from the disk slices in the longitudinal direction. Subsequently, they were ground and polished to a mirror finish using silicon carbide grinding papers and diamond suspension solutions before the final OPS polishing. To reveal the grains, the samples were electrolytically anodized at 20 VDC in a solution of H₂O + 3 pct HBF₄. A Neophot-31 optical microscope (made by Carl Zeiss, Jena, Germany) was used to take photos of the grain structure and a random linear intercept technique was applied to measure the grain size. Statistical analysis of the results was performed.

Results and Discussion

Grain refinement induced by UST prior to casting

Figure 2 displays a sequence of as-cast polarised micrographs taken at half radius of the DC-simulator billets for all experiments S1-S5 (Table II). One can see that the microstructure of the reference experiment S1 without grain refiner (Figure 2-a) consisted of big columnar grains > 1000 μ m (Figure 2-f). The lack of nuclei in this experiment failed to promote a Columnar to Equiaxed transition (CET) [24], [25].

On the other hand, when 0.1 wt.% Al-5Ti-1B grain refiner was added to the AA6082 melt before casting (S2), a completely equiaxed microstructure was obtained (Figure 2-b) and the grain size was reduced significantly down to 250 μ m (Figure 2-f). It is well known that an Al₃Ti

two-dimensional compound can adsorb on the TiB_2 particle making it a perfect seed for α -Al nucleation [26].

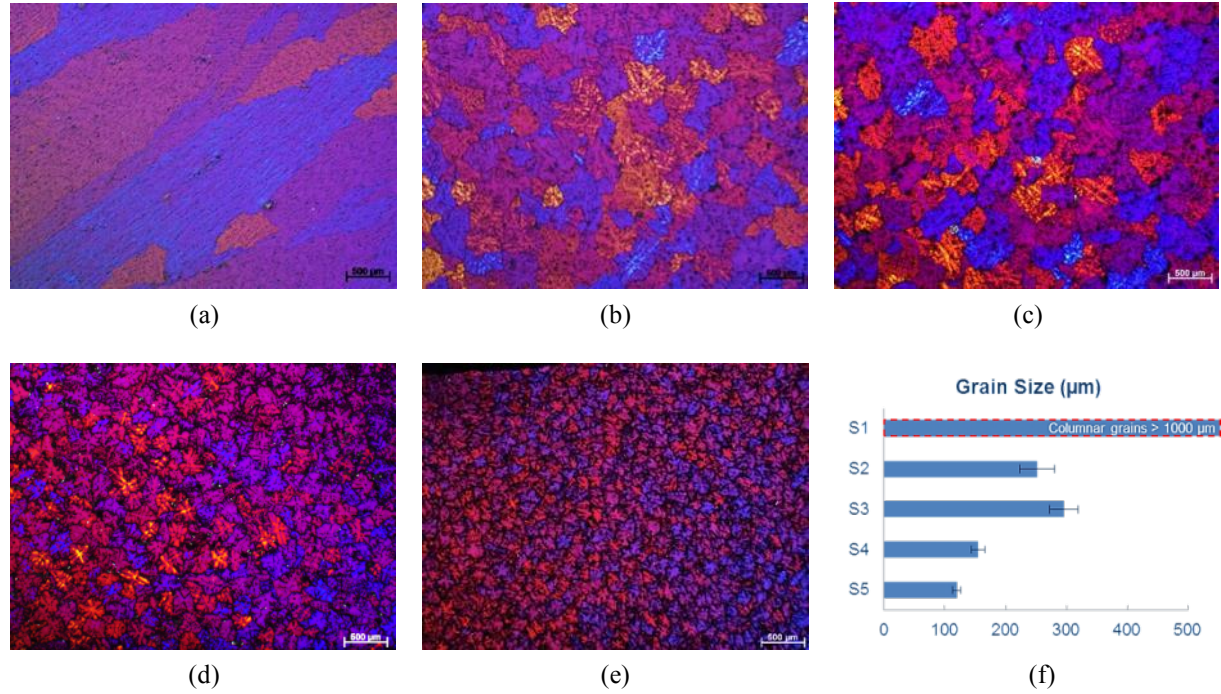


Figure 2: Micrographs showing the as-cast polarised microstructures revealing the grains obtained in the experiments (a) S1, (b) S2, (c) S3, (d) S4 and (e) S5. The grain size is plotted in (f), the error bar is the standard deviation obtained during the measurements.

In experiment S3, no commercial grain refiner was added but the concentrations of Zr and Ti were increased (see Table II). Figure 2-c shows that the microstructure obtained is fully equiaxed and comparable in size to that of experiment S2 (Figure -f). As a matter of fact, when the Zr content is increased to 0.2 wt.% in an AA6082 alloy, thermodynamic calculations using PandaT software show that an Al_3Zr intermetallic phase nucleates at a higher temperature ($T_{L(\text{Al}_3\text{Zr})} = 710 \text{ }^\circ\text{C}$) than that expected for the α -Al phase ($T_{L(\alpha\text{-Al})} = 650 \text{ }^\circ\text{C}$), thus forming primary particles. This Al_3Zr phase has been reported to be a nuclei for the α -Al phase especially when Ti is present [20], contributing to the grain refinement seen in experiment S3. In addition, the increase of Ti content to 0.1 wt.% in S3 increases significantly (by 20 points) the value of the growth restriction factor $Q_{\text{Ti}} = m_L(k-1)C_{\text{Ti}}$, where $m_L = 34 \text{ }^\circ\text{C}/\text{wt}\%$ is the liquidus slope, $k = 9.71$ the partition coefficient of a binary Al-Ti, and $C_{\text{Ti}} = 0.1 \text{ wt}\%$ is the composition of the Ti in experiment S3. It is well known that a large growth restriction factor will significantly reduce the grain size of a solidified material [11].

Figure 2-e shows the microstructure of the AA6082 material with 0.2 wt% Zr and 0.1 wt% Ti (S5), but after UST applied in the crucible in the temperature range of 750–705 °C before pouring in the DC-caster simulator. One can see that a fully equiaxed microstructure is achieved and a dramatic reduction in grain size down to $\sim 100 \text{ } \mu\text{m}$ is obtained (Figure 2-f). Similar to experiment S3 the high amount of Zr in the cast allows Al_3Zr to nucleate before the α -Al, therefore facilitating the nucleation of the latter and promoting CET. Also the high Ti content increases the growth restriction factor limiting the growth of the grains, which results in a small grain size. But clearly there is a significant reduction in the grain size between S3 and S5. This

can only be achieved due to the UST applied in the temperature range where the Al_3Zr intermetallics nucleate, resulting the multiplication of the Al_3Zr intermetallics and thus creating abundant potent nucleation sites for the $\alpha\text{-Al}$ phase to grow on.

By contrast, in experiment S4 with a lower concentration of Ti (Figure 2-d), the equiaxed grains have a larger size of $\sim 150\ \mu\text{m}$ compared to S5 (see Figure 2-f). This highlights the effect of Ti as a growth restrictor on the $\alpha\text{-Al}$ grains.

Figure 3 shows several micrographs at a magnification of $\times 20$ polarized imaging (Figure 3-a, b, c) and bright field $\times 100$ bright field imaging (Figure 3-d, e, f) revealing the intermetallics detected at the centre of the $\alpha\text{-Al}$ grains. These intermetallics were numerous in the microstructure and were observed in all three experiments S3 (Figure 3-a, d), S4 (Figure 3-b, e), and S5 (Figure 3-c, f) where the alloys contained 0.2 wt% Zr.

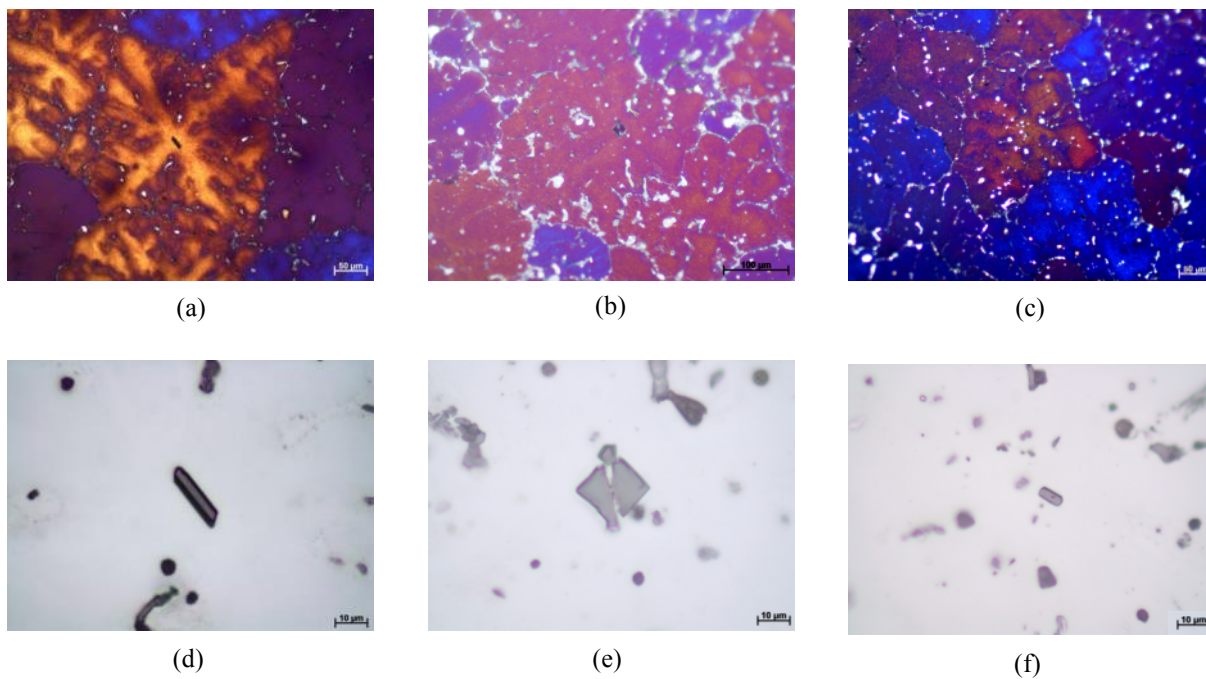


Figure 3: Micrographs showing the as-cast polarised micrographs (magnification $\times 20$) revealing the intermetallics detected at the centre of the grains in the experiments (a) S3, (b) S4, (c) S5. (d), (e) and (f) are bright field light micrographs at a magnification of $\times 100$ showing the same intermetallics detected in (a), (b) and (c) respectively.

Further SEM investigation of the sample S4 showed how the intermetallics were abundant and easy to find in the microstructure. In backscattered (BSE) mode, they appear as bright intermetallics in the image (Figure 4-a), with the bright colour indicating that they contain a higher concentration of heavy elements compared to aluminium.

Figure 4 shows an example of EDS mapping performed on multiple intermetallics. A mean EDS measurement was done in the blue rectangle indicated in Figure 4-b and reveals the intermetallic composition (Table III), thus the estimated stoichiometry is about $\text{Al}_3(\text{Zr}_{0.6}, \text{Ti}_{0.2}, \text{Si}_{0.2})$.

One can see from Figure 4-d,e that the Zr and Ti are homogeneously distributed in the intermetallics. This comes in line with the observation done by Atamanenko et al. [20], where he

found that the Zr and Ti are homogeneously distributed in the small intermetallics detected in an aluminium alloy with 0.6 wt.% Zr – 0.06 wt.% Ti alloy. They also found that the Ti content was between 3.6 and 6 at. pct. In addition, Figure 4-f shows that Si is present in the intermetallics and is homogeneously distributed in them with an atomic composition comparable to the Ti one.

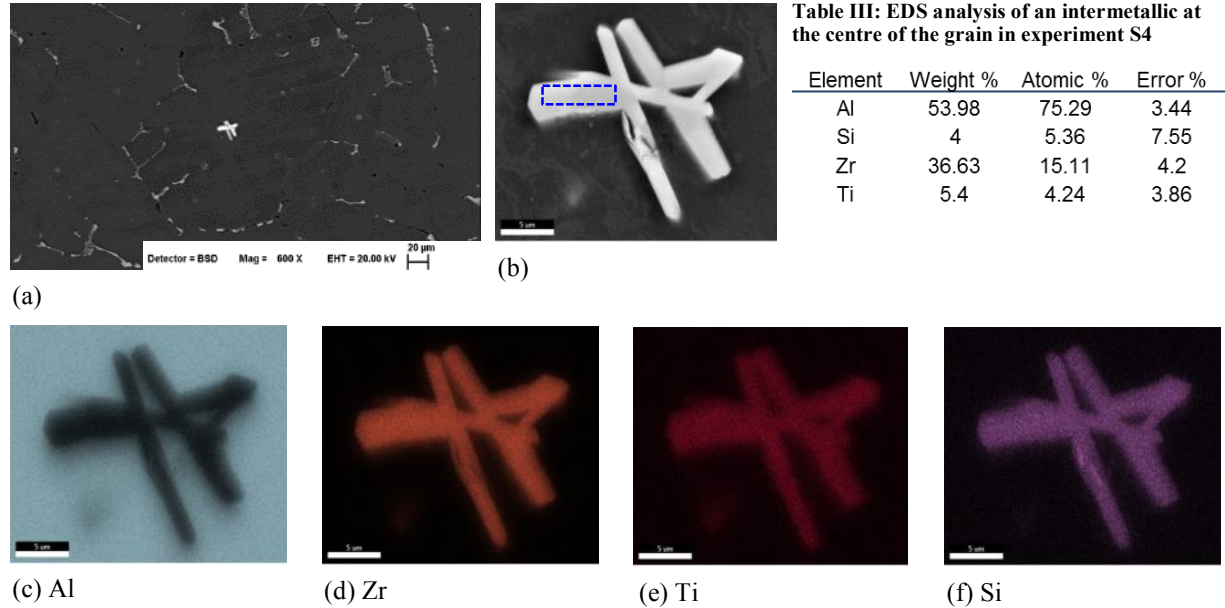


Figure 4: Scanning Electron Microscopy images of intermetallics detected at the centre of the α -Al grain in the experiment S4. The intermetallics appeared in bright white in the backscattered image at a magnification of x600 (a). (b) shows a secondary electron SEM image at a magnification of x10K, the blue rectangle indicates the region where the average EDS measurement was performed (Table III). EDS mapping reveals the (c) Al, (d) Zr, (e) Ti and (f) Si distributions in the intermetallics.

Conclusion

This work has proved that significant grain refinement of DC-cast 6082 commercial alloy can be achieved by applying ultrasonic melt treatment prior to casting on a Zr containing 6082 alloy without any commercial grain refiner addition. The Zr and Ti content required to achieve such a grain refinement are low enough to lie in the range of a commercial 6082. The temperature range where the UST is applied is crucial for the grain refinement because it needs to be in the interval where the Al_3Zr intermetallics nucleate. This technique is relatively easy to apply on a production line because there is no interference with the DC-caster, the UST is applied far from the sump prior to solidification. The next step is to perform additional SEM analyses on experiments S3 and S5 to detect any differences in the intermetallics detected at the centre of the grains in terms of stoichiometry or element distribution homogeneity. In addition, work is being carried out to validate the experiments on an 80 mm diameter conventional DC-caster.

Acknowledgments

The authors gratefully acknowledge all their colleagues at Constellium (especially E. Beslin) and BCAST (especially A. Fitzner, J. Gadd), for their support and technical help.

The authors wish to thank the Engineering and Physical Sciences Research Council (EPSRC) for funding the project.

References

- [1] D. G. Eskin, *Physical Metallurgy of Direct Chill Casting of Aluminum Alloys*. CRC Press, 2008.
- [2] M. Rappaz, J.-M. Drezet, and M. Gremaud, "A new hot-tearing criterion," *Metall. Mater. Trans. A*, vol. 30, no. 2, pp. 449–455.
- [3] G. Dobra, P. Moldovan, C. Stănică, G. Popescu, and M. Buțu, "Microporosity Formation in DC cast 5083 Alloy," *Light Met. TMS*, pp. 733–737, 2007.
- [4] M. Lalpoor, D. G. Eskin, D. Ruvalcaba, H. G. Fjær, A. Ten Cate, N. Ontijt, and L. Katgerman, "Cold cracking in DC-cast high strength aluminum alloy ingots: An intrinsic problem intensified by casting process parameters," *Mater. Sci. Eng. A*, vol. 528, no. 6, pp. 2831–2842, Mar. 2011.
- [5] R. Nadella, D. G. Eskin, Q. Du, and L. Katgerman, "Macrosegregation in direct-chill casting of aluminium alloys," *Prog. Mater. Sci.*, vol. 53, no. 3, pp. 421–480, Mar. 2008.
- [6] J. J. Favier, "Macrosegregation—I unified analysis during non-steady state solidification," *Acta Metall.*, vol. 29, no. 1, pp. 197–204, 1981.
- [7] D. G. McCartney, "Grain refining of aluminium and its alloys using inoculants," *Int. Mater. Rev.*, vol. 34, no. 1, pp. 247–260, Jan. 1989.
- [8] B. S. Murty, S. A. Kori, and M. Chakraborty, "Grain refinement of aluminium and its alloys by heterogeneous nucleation and alloying," *Int. Mater. Rev.*, vol. 47, no. 1, pp. 3–29, Feb. 2002.
- [9] K. A. Jackson, J. D. Hunt, D. R. Uhlmann, and T. P. Seward, "On Origin of Equiaxed Zone in Castings," *Trans. Metall. Soc. AIME*, vol. 236, p. 149, 1966.
- [10] H. Nguyen-Thi, G. Reinhart, N. Mangelinck-Noël, H. Jung, B. Billia, T. Schenk, J. Gastaldi, J. Härtwig, and J. Baruchel, "In-Situ and Real-Time Investigation of Columnar-to-Equiaxed Transition in Metallic Alloy," *Metall. Mater. Trans. A*, vol. 38, no. 7, pp. 1458–1464, Jul. 2007.
- [11] A. I. Greer, P. S. Cooper, M. W. Meredith, W. Schneider, P. Schumacher, J. A. Spittle, and A. Tronche, "Grain Refinement of Aluminium Alloys by Inoculation," *Adv. Eng. Mater.*, vol. 5, no. 1–2, pp. 81–91, Feb. 2003.
- [12] J. W. Fu and Y. S. Yang, "Microstructure and mechanical properties of Mg–Al–Zn alloy under a low-voltage pulsed magnetic field," *Mater. Lett.*, vol. 67, no. 1, pp. 252–255, Jan. 2012.
- [13] Y.-Y. Gong, J. Luo, J.-X. Jing, Z.-Q. Xia, and Q.-J. Zhai, "Structure refinement of pure aluminum by pulse magneto-oscillation," *Mater. Sci. Eng. A*, vol. 497, no. 1–2, pp. 147–152, Dec. 2008.

- [14] D. Liang, Z. Liang, Q. Zhai, G. Wang, and D. H. StJohn, "Nucleation and grain formation of pure Al under Pulsed Magneto-Oscillation treatment," *Mater. Lett.*, vol. 130, pp. 48–50, Sep. 2014.
- [15] X. Liao, Q. Zhai, J. Luo, W. Chen, and Y. Gong, "Refining mechanism of the electric current pulse on the solidification structure of pure aluminum," *Acta Mater.*, vol. 55, no. 9, pp. 3103–3109, May 2007.
- [16] V. Metan, K. Eigenfeld, D. Rübiger, M. Leonhardt, and S. Eckert, "Grain size control in Al–Si alloys by grain refinement and electromagnetic stirring," *J. Alloys Compd.*, vol. 487, no. 1–2, pp. 163–172, Nov. 2009.
- [17] D. Rübiger, Y. Zhang, V. Galindo, S. Franke, B. Willers, and S. Eckert, "The relevance of melt convection to grain refinement in Al–Si alloys solidified under the impact of electric currents," *Acta Mater.*, vol. 79, pp. 327–338, Oct. 2014.
- [18] Z. Fan, Y. Wang, M. Xia, and S. Arumuganathar, "Enhanced heterogeneous nucleation in AZ91D alloy by intensive melt shearing," *Acta Mater.*, vol. 57, no. 16, pp. 4891–4901, Sep. 2009.
- [19] G. I. Eskin and D. G. Eskin, *Ultrasonic Treatment of Light Alloy Melts*. Boca Raton: CRC Press, 2014.
- [20] T. V. Atamanenko, D. G. Eskin, L. Zhang, and L. Katgerman, "Criteria of grain refinement induced by ultrasonic melt treatment of aluminum alloys containing Zr and Ti," *Metall. Mater. Trans. A*, vol. 41, no. 8, pp. 2056–2066, Aug. 2010.
- [21] G. Wang, M. S. Dargusch, M. Qian, D. G. Eskin, and D. H. StJohn, "The role of ultrasonic treatment in refining the as-cast grain structure during the solidification of an Al–2Cu alloy," *J. Cryst. Growth*, vol. 408, pp. 119–124, Dec. 2014.
- [22] L. Zhang, D. G. Eskin, and L. Katgerman, "Influence of ultrasonic melt treatment on the formation of primary intermetallics and related grain refinement in aluminum alloys," *J. Mater. Sci.*, vol. 46, no. 15, pp. 5252–5259, Aug. 2011.
- [23] H. T. Li, S. Ji, Y. Wang, M. Xia, and Z. Fan, "Effect of intensive melt shearing on the formation of Fe-containing intermetallics in LM24 Al-alloy," *IOP Conf. Ser. Mater. Sci. Eng.*, vol. 27, p. 12075, Jan. 2012.
- [24] H. Jung, N. Mangelinck-Noël, H. Nguyen-Thi, B. Billia, G. Reinhart, and A. Buffet, "Directional solidification processing on CET in Al-based alloys," *Met. Mater. Int.*, vol. 15, no. 1, pp. 21–26, Feb. 2009.
- [25] G. Reinhart, H. Nguyen-Thi, N. Mangelinck-Noël, B. Billia, T. Schenk, and J. Baruchel, "CET during the solidification of refined Al-3.5wt%Ni alloys and characterization of the subsequent grain structure," *IOP Conf. Ser. Mater. Sci. Eng.*, vol. 27, p. 12011, Jan. 2012.
- [26] Z. Fan, Y. Wang, Y. Zhang, T. Qin, X. R. Zhou, G. E. Thompson, T. Pennycook, and T. Hashimoto, "Grain refining mechanism in the Al/Al–Ti–B system," *Acta Mater.*, vol. 84, pp. 292–304, Feb. 2015.